

# Kepler observations of flaring in A–F type stars

L. A. Balona<sup>★</sup>

South African Astronomical Observatory, PO Box 9, Observatory 7935, Cape Town, South Africa

Accepted 2012 April 19. Received 2012 April 18; in original form 2012 March 23

## ABSTRACT

Optical flares on early F- and A-type stars have never been observed with certainty. Inspection of several thousands of these stars in the *Kepler* public archives resulted in the discovery of flares in 25 G-type and 27 F-type stars. Because A-type stars are thought not to be active, the detection of flares on 19 A-type stars from a sample of nearly 2000 A stars is particularly noteworthy. The flares have relative intensities in the range 1–100 parts per thousand and typical durations of a few minutes to several hours. The mean interval between flares varies between 1 and 120 days. We estimate the typical energy of flares to be around  $10^{35}$  erg in the F-type stars and about  $10^{36}$  erg in the A-type stars. Nearly all these stars vary at a low level with a period which is most likely the rotational period of the star. Comparison of the relative flare intensities with those in cool red stars observed by *Kepler* shows that flares in these stars, and certainly in the A-type stars, cannot easily be ascribed to cool flare-star companions. The huge energy released in the flares is difficult to understand. This is especially the case for A-type stars since these stars are thought to have very weak magnetic fields. The flare energy may possibly originate in magnetic reconnection of field lines between the primary star and a companion.

**Key words:** stars: activity – stars: flare – starspots.

## 1 INTRODUCTION

Stellar flares are usually associated with active M dwarfs – the UV Ceti variables. These stars can dramatically increase in brightness over a broad wavelength range from X-rays to radio waves for anywhere from a few minutes to a few hours. The rapid rise in brightness is followed by a slow decay with a time-scale from minutes to hours. The largest change in brightness occurs at short wavelengths: a rise of one magnitude in the *V* band is typically accompanied by a rise of five magnitudes in the *U* band. During a flare, the Balmer lines are in emission and the spectrum of ionized helium makes an appearance.

Flares in the Sun are caused by energy released by the reconnection of magnetic field lines in the outer atmosphere. During these events, energetic particles are accelerated deeper into the atmosphere, resulting in emission from X-rays to radio waves (Benz & Güdel 2010). Flares in active M dwarfs are typically 10–1000 times more energetic than solar flares (Güdel & Nazé 2009) and are qualitatively different in several respects. Although we have very limited understanding of these flares, it is thought that the underlying mechanism is essentially the same as in the Sun.

The RS CVn variables are a class of detached binaries typically composed of a chromospherically active G or K star. Tidal locking

in these stars ensures that the rotational period is the same as the orbital period, which ranges from a few days to as long as one month. The RS CVn binaries display a high level of activity with strong chromospheric line emissions. These stars show rotational modulation of photospheric spots and are magnetically active. Flares in RS CVn stars have been mostly detected in X-rays, though optical flares have been observed (Mathioudakis et al. 1992). There is some evidence to suggest that flaring is associated with spots, as it is in the Sun. A magnetic field connecting the two stars has the potential for releasing enormous amounts of energy and may be a source of flaring in these stars (Simon, Linsky & Schiffer 1980; van den Oord 1988; Gunn et al. 1997). We do not yet know the precise mechanism, though it is generally accepted that the flare energy is derived in some way from the magnetic field.

Schaefer (1989) discusses ‘flashes’ in 24 normal main-sequence K–B type stars. These are unique events detected in a variety of ways where the brightness of the star was observed to increase on time-scales of seconds to hours and by a fraction of a magnitude to several magnitudes. Schaefer argues that these ‘superflares’ may be intrinsic to the star (a ‘superflare’ is a term used by Rubenstein & Schaefer (2000) and others for a flare with an energy exceeding  $10^{33}$  erg). Schaefer, King & Deliyannis (2000) have identified nine cases of superflares on normal solar-type stars on or near the main sequence with spectral types in the range F8–G8. These identifications are mostly from historical photographic and photoelectric photometry. The stars appear to be single and not very rapidly rotating or very

<sup>★</sup>E-mail: lab@saao.ac.za

young. Schaefer (1991) discusses 14 cases of flares detected in Mira variables. Wang (1993) reported a flare on the A5–A7 star BD+47°819 which brightened from 10.0 to 8.5 mag in the *U* band.

Typical solar flares have energies of about  $10^{29}$  erg, while the most energetic solar flares are about  $10^{31}$  erg. The superflares are estimated to have energies in the range  $10^{35}$ – $10^{39}$  erg. Such a large release of energy is difficult to understand. Rubenstein & Schaefer (2000) suggest that superflares may be caused by magnetic reconnection in magnetic field lines connecting the star with a planet. However, Ip, Kopp & Hu (2004) suggest that this energy may only reach the level of a typical solar flare. The influence of a close planet on stellar activity has been discussed by Cuntz, Saar & Musielak (2000) and Lanza (2008).

Flaring in the extreme ultraviolet has been detected in HR 120 (F2V) and 71 Tau (F0V, A8n) (Mullan & Mathioudakis 2000). An intense X-ray flare was observed in HD 161804 (A1IV/V) (Miura et al. 2008) which is attributed to the interaction of the A star with an unseen cooler companion. X-ray flaring also occurs in the A2Vn star Castor A (Schmitt, Guedel & Predehl 1994) and seems to be intrinsic to the A star and not to a late-type companion. Schröder & Schmitt (2007) found a total of 312 bright A-type stars positionally associated with *ROSAT* X-ray sources. They attribute the X-ray emission from these stars, without much doubt, to late-type companions. More recently, Robrade & Schmitt (2011) found X-ray emission in two A0p stars, IQ Aur and  $\alpha^2$  CVn, including an X-ray flare in IQ Aur. The rapidly rotating bright A7V star Altair is a source of X-rays which could be a result of a dynamo mechanism operating in the cool equatorial region (Robrade & Schmitt 2009). Another example is the Am star HR 8799 (kA5hF0mA5) which is a weak soft X-ray emitter (Robrade & Schmitt 2010).

Flaring is also present in B-type stars. The late B-type main-sequence star HD 38563S as well as HD 261902 (B8) and HD 47777 (B3) show clear flare-like time variations in X-rays (Yanagida, Ezoe & Makishima 2004; Yanagida et al. 2007). The X-ray activity in late B stars is thought to be intrinsic to the stars themselves and not in a cool companion (Berghoefter & Schmitt 1994). However, in some cases at least, active cool companions may be responsible (Hubrig et al. 2007).

While flares in cool stars are thought to be a result of magnetic energy release, X-ray flaring emission in early B-type stars probably arises from shocks and instabilities in their radiatively driven winds. X-ray emission should stop around B5–B8 when radiation pressure becomes negligible. Neither wind instabilities nor magnetic energy release can account for flaring in stars with spectral types in the range F5–B5. The A-type stars should therefore neither have flares nor be X-ray sources. The overall X-ray detection rate among these stars is around 10–15 per cent, which is indeed quite low (Schröder & Schmitt 2007), but not negligible. The detection rate increases steeply for F-type stars.

The prevailing view is that only stars with a sufficiently deep surface convective zone can generate a magnetic field through dynamo activity. The presence of a magnetic field is required for flaring. The magnetic field also leads to the development of starspots. There is therefore an association between flares and starspots in cool stars. In the Sun, for instance, nearly all flares occur in or close to sunspots. The more magnetically active the sunspot group, the greater the frequency of flaring (Bell & Glazer 1959). The magnetic field must be sufficiently strong to suppress the overturning convective motion. The energy flow from the interior is therefore reduced, resulting in the formation of a locally cool and dark region (Biermann 1948). The mechanism just described can only operate for stars cooler than about F5 which have a sufficiently deep convective envelope.

No spotted star earlier than about F8 has been detected with certainty. Starspots that have been observed are in general much larger than those on the Sun, covering as much as 30 per cent of the stellar surface. Simulations suggest that these very large spots can be of significantly different appearance and not easily explained as scaled versions of sunspots, even for stars similar to the Sun (Strassmeier 2009).

The advent of high-precision photometry from space has led to a number of unexpected discoveries regarding stellar activity. For example, *CoRoT* observations of a few B stars seem to be more easily explained by a spot model than by stellar pulsation (Degroote et al. 2009). In these stars the resemblance to simulated light curves of rotating spotted stars (e.g. Strassmeier & Bopp 1992; Lanza, Rodono & Zappala 1993) is apparent. Inspection of *Kepler* light curves of A–F stars shows that most of these stars are variable at low frequencies (Balona 2011). The period of variability is consistent with the rotation period, with the possibility that at least some of the variation could be due to starspots. Indeed, Balona (2011) finds that about 8 per cent of *Kepler* A-type stars show light curves strongly resembling migrating starspots, just like those seen in the *CoRoT* B stars (Degroote et al. 2009). Many more A-type stars show quasi-periodic light variations of variable amplitude which may perhaps be attributed to changing starspots. Since there appears to be a close association between spots and flares, the possibility exists of detecting flares in these hot stars.

Solar white-light flares (WLFs) are a rare type of flare that results in an increase in the optical continuum or integrated light. Kretzschmar (2011) has presented evidence that all flares are WLFs and that the white-light continuum is the main contributor to the total radiated energy of the flare. The detection of WLFs is difficult because the increase in continuum brightness is not detectable except for the largest flares. The WLF spectrum is consistent with a blackbody emission at about 9000 K. Analysis of several flare events in white light shows that if the Sun were to be observed as a star, the strongest flares would show a maximum relative brightness increase of only about  $2 \times 10^{-5}$  and the weaker, more common, flares about  $2 \times 10^{-6}$ . Since the solar radiated power is  $3.8 \times 10^{33}$  erg s<sup>-1</sup> and a typical flare has a duration of around  $2 \times 10^3$  s, these relative brightnesses imply flare energies around  $10^{30}$ – $10^{31}$  erg, which is typical of the most energetic solar flares.

The *Kepler* space mission has provided an exceptional data base for the study of cool flare stars. Walkowicz et al. (2011) present results of a search for flares in 373 cool dwarfs observed by *Kepler*. They calculate relative flare energies, flare rates and durations. By contrast to the large brightness variation in the blue region, in the white-light passband used by *Kepler* the typical increase in relative brightness during the largest flare is only about  $3 \times 10^{-3}$ . The typical duration is 3–5 h with flaring occurring every few days. The flares in these *Kepler* M–K dwarfs are the equivalent of WLFs in the Sun.

The results discussed above serve to show that stellar flares may not be the exclusive domain of cool red dwarfs, but could be present in all stars, even the A- and late B-type stars. While it is possible to attribute flaring in these stars to a late-type companion, this may not always be the case. The possible detection of starspots in A- and late B-type stars and the known link between flaring and spots increase the likelihood that at least some flares may be intrinsic to these stars.

Our aim in this paper is to bring attention to some stars which, according to the *Kepler* Input Catalogue (KIC; Brown et al. 2011), are G-, F- or A-type stars but which show evidence of flare-like activity. These stars came to light through visual inspection of the

light curves of over 10 000 stars observed by *Kepler*. None of the stars in this sample is common to the much cooler sample of *Kepler* flare stars observed by Walkowicz et al. (2011).

## 2 THE DATA

The *Kepler* satellite is in a 370-d orbit around the Sun. It has observed, and continues to observe, several hundred thousand stars with a photometric precision in the micromagnitude region. Most of these observations were obtained in the long-cadence (LC) mode with integration times of 29.4 min (Jenkins et al. 2010). A smaller number of stars were observed in the short-cadence (SC) mode with sampling times just under 1 min (Gilliland et al. 2010). The data are downloaded every quarter of the orbital period when the solar panels are repositioned. The data are available in ‘uncalibrated’ or ‘calibrated’ form. The calibrated data suffer from artefacts caused by the processing and is not used here. All the data used in this paper are publically available and can be retrieved using Multimission Archive at the Space Telescope Science Institute. All stars were observed in the LC mode, the data being mostly from quarters 0 to 6. Quarter 0 is a commissioning run lasting only 10 days; the other quarters have a duration of about 90 days. The SC data nearly all have a duration of about 30 days.

We inspected the light curves of over 10 000 stars, mostly with  $T_{\text{eff}} > 5000$  K, employing a classification based on the visual appearance of the light curves and periodograms (Balona 2011). In the process we noted many flare-like events in the raw light curves.

Naturally, some of these events are of instrumental origin. We eliminated events which occurred at the same time in different stars within a window of 0.1 d. These simultaneous events are certainly of instrumental origin. From more than 2700 flare-like events, only 109 (4 per cent) were eliminated using this criterion. In this paper, we list all stars where at least one flare was noticed in the sample of over 10 000 *Kepler* stars.

Identification of flares from SC observations is based on the rapid rise and slow decay that one expects from a flare. All flares detected from SC observations have this characteristic shape. However, only the brightest flares observed in the LC mode are resolved. The long exposure time also greatly reduces the peak brightness, making flares more difficult to detect in this mode. In some stars observed in the LC mode, we infer the presence of flares through repeated sudden brightenings, even though none of the flares are fully resolved. Although we feel confident that these are very likely flare events, the lack of time resolution certainly renders them less convincing.

The stars for which at least one flare-like event was detected are listed in Tables 1–4. In these tables, we present the photometric equivalent width (EW) of the largest flare as described in Walkowicz et al. (2011). Also shown is the peak relative increase in brightness and the total duration of the flare. We also list the duration at the flare at half the peak value. Stars have been classified into spectral-type groups G9–F9, F9–F5, F5–A8 and A8–A0 depending on the KIC effective temperature. Pinsonneault et al. (2012) have re-examined the KIC temperature scale and find that the temperatures are too

**Table 1.** List of flare stars with temperature range corresponding to spectral types G9–F9. The second column lists the cadence used (L: long cadence; S: short cadence). This is followed by the *Kepler* magnitude, Kp, the effective temperature (in K) and surface gravity ( $\text{cm s}^{-2}$ ) from the KIC. The number of flares,  $N$ , in the LC data and the typical interval between flares,  $\tau$  (in days), are given. The integrated flux of the largest flare is given by  $\text{EW}_{\text{phot}}$  (hours). The peak relative flux is  $\Delta F/F$  and  $\Delta t$  is the total duration (hours), while FWHM is the full width at half-maximum (hours). The presumed rotation period (days) is derived from the light curve. In the notes ECL means an eclipsing binary and X-ray means an X-ray source.

KIC	Cad	Kp (mag)	$T_{\text{eff}}$ (K)	$\log g$	$N$	$\tau$ (d)	$\log \text{EW}$ (h)	$\log \Delta F/F$	$\Delta t$ (h)	FWHM (h)	Period (d)	Notes
3626094	L	11.099	5835	4.3	35	13.6	−2.359	−2.436	2.452	0.490	0.72	
4742436	SL	10.600	5628	4.1	53	9.1	−3.334	−2.624	0.523	0.196	2.33	
4831454	SL	10.690	5298	4.6	21	22.1	−2.778	−2.026	0.768	0.049	5.18	
5475645	SL	11.205	5336	4.7	67	7.4	−1.489	−1.568	5.509	0.572	15.34	
5733906	SL	11.839	5241	3.7	14	28.6	−2.054	−1.642	1.373	0.229	0.72	
6470892	L	11.866	5819	3.8	48	10.4	−2.747	−2.883	4.904	0.490	7.68	
6677144	SL	11.391	5561	4.4	24	20.0	−2.342	−2.763	6.866	1.471	–	
7264976	L	11.974	5184	4.1	128	3.8	−0.768	−1.221	12.751	0.490	12.64	
7420545	SL	9.996	5083	3.8	45	11.3	−2.101	−2.374	7.944	0.687	18.14	
7552212	L	11.711	5510	4.4	11	28.8	−2.543	−2.729	2.943	0.490	3.39	
7751017	L	11.965	5665	4.3	54	9.4	−2.875	−2.785	1.471	0.490	3.65	$\gamma$ Dor?
8226464	SL	11.468	5754	4.0	108	4.5	−1.462	−1.663	5.182	1.569	3.10	
8915957	SL	10.918	5254	3.5	12	39.1	−2.397	−2.368	3.057	0.817	7.69	
9077192	L	14.468	4746	4.4	81	6.2	−0.776	−1.350	15.202	1.962	1.15	
9412514	SL	11.391	5958	4.2	15	31.6	−2.902	−2.881	0.229	0.213	3.70	
9582720	L	12.652	5618	4.5	42	11.9	−1.702	−1.820	4.904	0.490	1.50	
9655134	SL	13.632	5229	4.5	77	10.8	−2.293	−2.208	0.768	0.262	13.69	
9833666	SL	9.680	5411	3.7	106	4.8	−2.106	−2.465	4.757	2.942	10.26	
10004510	L	14.192	4341	4.6	105	4.8	−0.118	−0.208	8.337	0.490	1.37	
10063343	SL	13.164	3976	4.4	87	9.7	−1.102	−0.312	0.703	0.098	0.33	
10448382	SL	11.447	5979	4.3	33	14.1	−2.491	−2.298	1.962	0.981	2.19	
10453475	L	14.191	5202	4.5	57	8.6	−0.303	−0.900	29.914	1.962	7.61	
10459987	SL	10.625	5018	4.7	134	3.7	−2.552	−1.958	1.340	0.098	6.02	
11551430	SL	10.691	5335	3.7	179	1.0	−1.404	−1.471	5.362	0.752	4.19	X-ray
11560431	SL	9.694	5094	4.5	99	1.1	−1.908	−1.647	3.139	0.311	3.14	X-ray

**Table 2.** The same as Table 1 but for stars in the temperature range corresponding to spectral types F9–F5.

KIC	Cad	Kp (mag)	$T_{\text{eff}}$ (K)	$\log g$	$N$	$\tau$ (d)	$\log \text{EW}$ (h)	$\log \Delta F/F$	$\Delta t$ (h)	FWHM (h)	Period (d)	Notes
2557430	SL	11.471	6248	4.1	8	72.8	-2.093	-1.814	1.700	0.294	1.30	ECL
3455586	L	11.546	6478	4.0	4	97.6	-2.439	-2.834	4.904	1.471	1.34	
5018442	SL	11.109	6012	4.2	36	11.6	-3.216	-2.651	0.621	0.213	0.51	$\gamma$ Dor?
5263749	SL	11.527	6347	4.0	6	30.9	-3.564	-2.685	0.474	0.147	3.73	ECL?
6545986	SL	10.983	6157	4.3	3	74.6	-2.750	-2.215	1.553	0.114	0.56	
6786176	SL	11.134	6211	4.0	20	22.4	-3.014	-2.324	0.638	0.114	-	
6791060	SL	10.477	6368	4.3	9	47.5	-3.244	-2.751	0.539	0.180	0.34	
7093428	SL	11.035	6057	4.2	152	3.3	-2.962	-1.830	0.507	0.049	0.51	
7820035	SL	11.546	6014	4.3	72	6.9	-3.584	-2.449	0.278	0.065	0.42	
8508009	SL	11.460	6024	4.1	16	8.2	-3.637	-2.506	0.245	0.098	2.95	
8838457	SL	11.199	6203	3.8	20	15.0	-3.247	-2.318	0.425	0.033	0.44	$\gamma$ Dor?
9902554	L	10.866	6237	4.1	61	8.1	-2.452	-2.512	5.885	0.490	4.72	
9946017	SL	11.146	6481	3.7	44	11.0	-1.956	-1.823	2.321	0.507	1.43	F5V
10355856	SL	9.195	6288	4.0	31	22.5	-2.499	-1.960	1.913	0.163	4.49	
11137395	SL	10.624	6064	4.2	20	23.9	-2.416	-1.923	1.471	0.163	1.57	X-ray
11507705	SL	11.635	6344	4.3	17	26.0	-3.134	-2.207	0.490	0.049	-	

**Table 3.** The same as Table 1 but for stars in the temperature range corresponding to spectral types F5–A8.

KIC	Cad	Kp (mag)	$T_{\text{eff}}$ (K)	$\log g$	$N$	$\tau$ (d)	$\log \text{EW}$ (h)	$\log \Delta F/F$	$\Delta t$ (h)	FWHM (h)	Period (d)	Notes
4568729	SL	11.521	6927	4.1	4	17.0	-2.920	-2.534	0.670	0.213	1.74	
4908893	SL	10.975	6795	3.9	9	28.8	-3.444	-2.562	0.229	0.065	1.62	
5870686	SL	9.909	7524	3.8	26	19.3	-4.120	-2.841	0.131	0.016	0.75	
6185416	SL	11.220	6636	4.2	33	15.3	-2.919	-2.372	0.638	0.213	2.06	
6957185	L	13.063	6514	4.1	14	31.6	-1.703	-1.795	2.452	0.490	0.75	
8505928	L	12.452	6546	4.2	4	64.9	-2.231	-2.259	4.904	0.490	2.04	
9206046	L	13.853	7293	4.0	12	37.3	-0.847	-1.283	6.866	1.471	2.12	
9778156	L	13.415	6633	4.1	61	7.8	-3.053	-2.729	1.962	0.490	3.34	
9881909	SL	11.424	6812	3.8	9	40.2	-2.769	-2.406	1.161	0.458	0.51	
9944208	L	14.194	7039	4.3	26	17.9	-1.248	-1.406	4.904	0.490	1.87	
11027270	SL	11.299	6846	3.9	11	45.4	-3.508	-2.372	0.278	0.049	0.42	

cool by about 100 K for stars in the region 6000–7000 K. The KIC effective temperatures are unreliable for B stars and the hotter A stars. Some stars in Table 4 are probably B-type stars.

It should be noted that there is no certainty of what constitutes a flare. As already mentioned, these events were noted simply by visual inspection of the light curves and are subjective in nature. Undoubtedly, some flares may turn out to be noise, and the number of flares listed in the tables must be taken merely as a rough indication. However, there is little doubt that the strongest flares are real, even in the LC data where the poor time resolution often does not allow us to distinguish the exponential decay which was taken as the hallmark of a genuine flare.

Figs 1–4 show examples of flares from the SC data. The SC data, of course, offer good time resolution, but due to the limited duration (usually no more than 30 d) there is a smaller chance of detection than in the longer LC data. For comparison, in Figs 5 and 6 we show flares in the LC data. For each star, three flares are shown to give an indication of the variety among the most easily distinguished flares.

In Table 5, we show the total number of stars searched in each temperature range and the number of flare stars in that range. For some unknown reason, there is a sharp drop in the relative number of flare stars for F5–A8.

One of the surprises in this work was that in all but three stars where flares are seen there is clear evidence of periodic variability (see Fig. 7). In most stars, one can detect first and second harmonics

of the main frequency and a strong variation in amplitude and shape of the light curve. It is difficult to understand this periodic low-amplitude variation in any way other than starspots. Whenever possible, we have noted this period in Tables 1–4. In a few stars one can detect a secondary wave which travels through the main variation slowly with time. This is a classic signature of migrating starspots.

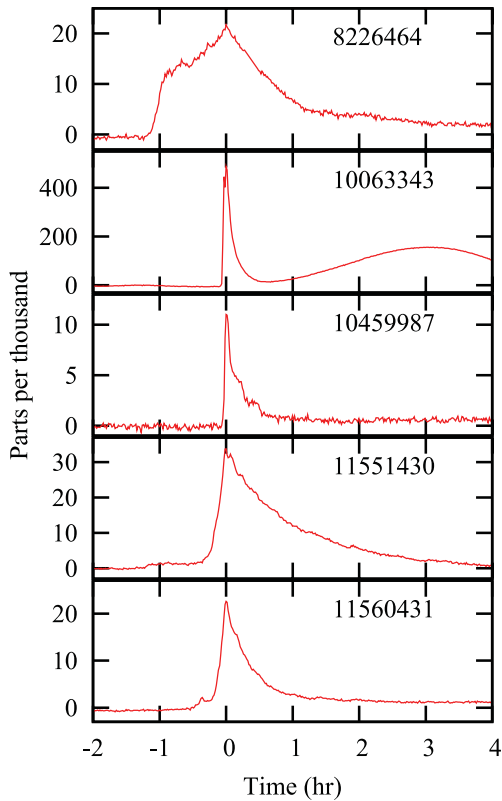
### 3 STARS OF PARTICULAR INTEREST

The A–F stars discussed here include stars within the  $\delta$  Scuti and  $\gamma$  Doradus instability strips. KIC 5898780 appears to be a  $\delta$  Sct variable with six or seven scattered frequencies in the range 4–10 d<sup>-1</sup> and amplitudes generally below 0.05 mmag. The dominant period of 3.16 d has variable amplitude which attains a peak-to-peak value of 2 mmag. The light curve changes shape with time. Although only LC data are available, a few very strong flares are resolved. It is particularly difficult to detect flares in  $\delta$  Sct and other stars with rapid light variations.

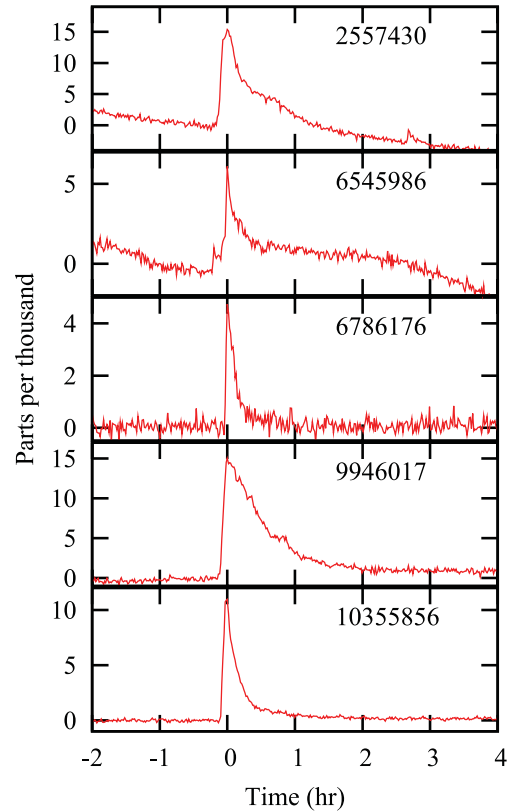
The light curves of *Kepler* stars presumed to be  $\gamma$  Dor variables have been discussed by Balona et al. (2011). They find three types of light curve which are probably associated with these variables. There is an asymmetric type with one dominant period and beats which seems to arise from non-linearities due to large pulsation amplitude. Another type shows multiple periods. Both these

**Table 4.** The same as Table 1 but for stars in the temperature range corresponding to spectral types A8–A0.

KIC	Cad	Kp (mag)	$T_{\text{eff}}$ (K)	log $g$	$N$	$\tau$ (d)	log EW (h)	log $\Delta F/F$	$\Delta t$ (h)	FWHM (h)	Period (d)	Notes
3974751	L	11.440	9265	4.1	60	6.5	-2.969	-2.994	4.414	2.207	2.48	HD 225660
4472809	L	13.989	8440	3.8	3	120.0	-1.842	-2.118	5.885	0.981	2.36	ECL
4773133	L	12.082	9383	4.2	2	–	-2.653	-3.085	6.866	1.962	0.49	
5113797	SL	9.152	8139	3.8	24	28.9	-2.602	-2.347	1.602	0.458	0.35	HD 225447, $\gamma$ Dor?
5201872	SL	9.480	7937	3.9	4	69.2	-2.878	-2.286	0.964	0.163	0.66	HD 225493, A2
5213466	L	13.075	8312	3.7	14	27.4	-2.346	-2.434	2.452	0.981	2.82	ECL
5559516	L	8.711	9309	4.1	5	75.2	-0.366	-3.114	0.981	0.490	5.73	HD 188283
5898780	L	12.777	8527	4.1	8	56.6	-2.136	-2.082	3.923	1.962	3.16	$\delta$ Sct?
6451234	L	12.766	8115	4.1	4	105.8	-2.782	-2.651	1.962	0.981	1.42	
7097723	L	11.679	8438	3.8	11	36.5	-1.344	-1.478	3.433	0.490	1.91	
7978512	L	12.287	9330	4.1	21	19.5	-2.697	-2.844	2.943	0.490	0.46	
8142623	SL	17.298	9332	4.1	48	17.5	-1.476	-1.004	0.490	0.294	1.12	sdB
8351193	SL	7.598	8467	4.0	14	56.0	-3.572	-3.460	1.389	0.719	0.57	HD 177152, B9V
8686824	L	10.682	8991	3.5	30	21.0	-2.735	-2.905	3.923	0.490	2.48	A3
8703413	SL	8.712	7713	3.8	8	60.0	-3.838	-3.089	0.343	0.082	6.54	HD 187254, A2m, X-ray
9216367	SL	12.119	7840	3.7	31	13.7	-2.957	-2.516	0.768	0.360	3.25	A2p:
10082844	L	13.693	9426	4.1	7	61.7	-1.761	-2.168	5.394	1.471	2.08	
10489286	L	11.836	8394	3.9	63	7.9	-2.632	-2.898	4.904	0.981	1.54	
10593239	SL	15.276	8259	3.9	68	11.7	-1.903	-1.818	1.962	1.128	1.89	sdB+F/G
10971633	L	11.461	9016	3.9	7	63.4	-2.613	-2.894	2.942	1.471	3.98	ECL
11189959	SL	8.212	9258	4.1	38	22.1	-3.839	-3.910	1.471	0.736	0.82	HD 183257, A0, X-ray
11350152	SL	15.490	8878	3.9	29	24.8	-2.487	-1.899	0.278	0.229	3.16	sdB+F/G

**Figure 1.** Examples of flares in some G9–F9 stars from the SC data. Relative intensities are in parts per thousand and the time is in hours.

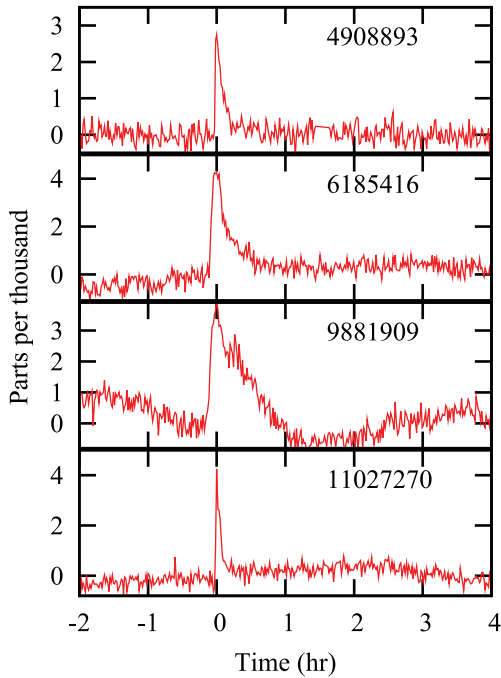
types are almost certainly due to  $\gamma$  Dor pulsation. By far the most common type has a dominant period with a symmetric light curve and beats. This latter type closely resembles the light curve associated with starspots. It is therefore not possible to discriminate

**Figure 2.** Examples of flares in some F9–F5 stars from the SC data.

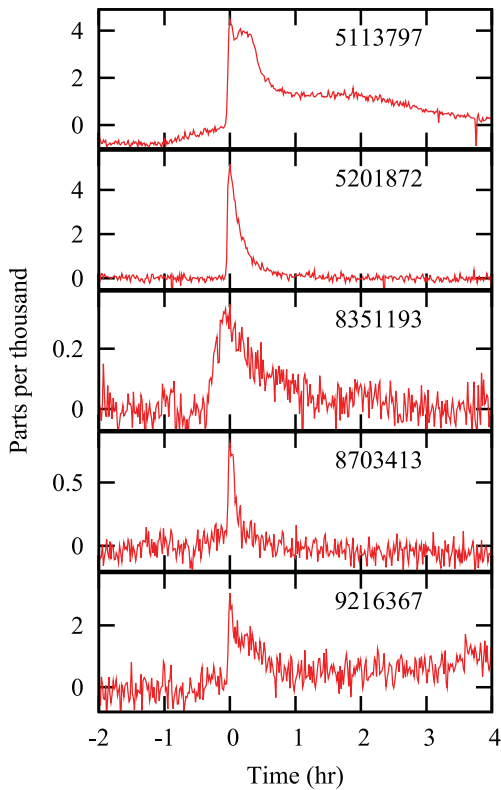
between  $\gamma$  Dor variables with symmetric light curves and rotational modulation due to starspots. Among stars of this type are KIC 5018442, KIC 5113797, KIC 7751017 and KIC 8838457.

The periodogram of KIC 5018442 shows two main frequencies, 0.51 and 0.36 d<sup>-1</sup>, and their harmonics. The peaks in the



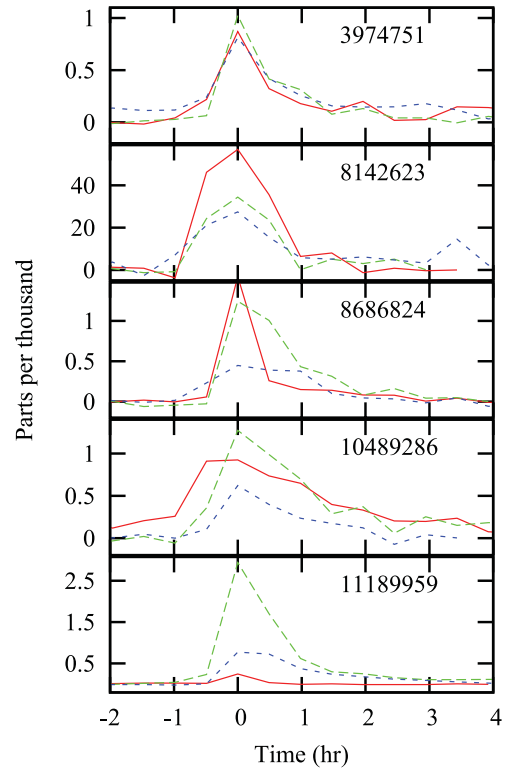


**Figure 3.** Examples of flares in some F5–A8 stars from the SC data.

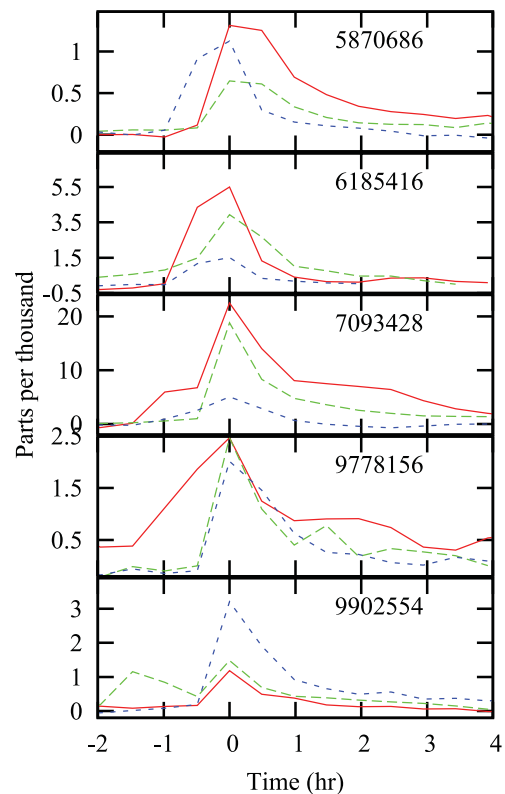


**Figure 4.** Examples of flares in some A8–A0 stars from the SC data.

periodogram are broad, suggesting stochastic behaviour. The SC data show one very clear large flare, but nothing obvious can be seen in the LC data, possibly because of the poor time resolution. KIC 7751017 has a period of 3.65 d with highly variable amplitude (7–45 mmag) and changing pulse shape. The SC data are not available, but the LC data show some partly resolved weak flares. In



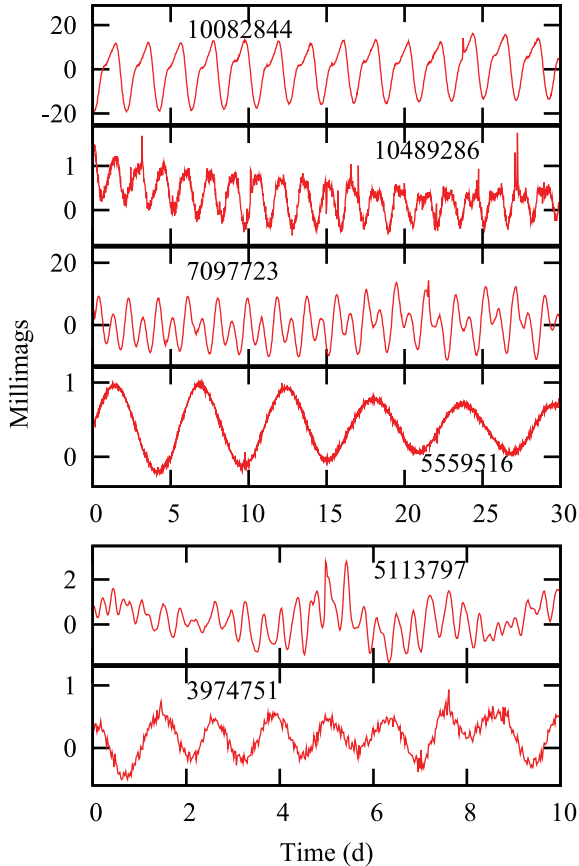
**Figure 5.** The LC data of some A8–A0 stars showing three different flares in each star.



**Figure 6.** The LC data of some F9–A8 stars showing three different flares in each star.

**Table 5.** Total number of stars searched in various spectral type ranges, the number of stars with flares and the percentage of flare stars.

$T_{\text{eff}}$ range	Sp. type	Total	Flare	Per cent
$5000 < T_{\text{eff}} < 6000$	G9–F9	2393	25	1.04
$6000 < T_{\text{eff}} < 6500$	F9–F5	1509	16	1.06
$6500 < T_{\text{eff}} < 7500$	F5–A8	5254	11	0.21
$7500 < T_{\text{eff}} < 10000$	A8–A0	1883	22	1.17

**Figure 7.** Partial light curves of some A8–A0 stars showing variable amplitudes and shapes characteristic of starspots.

KIC 8838457, the SC data show three moderate short-lived flares. The LC data show one strong resolved flare and several weaker unresolved flares. The light curve has variable amplitude in the range 1.5–3.0 mmag and a period of 0.443 d. The star is classified as a  $\gamma$  Dor variable by Uytterhoeven et al. (2011).

KIC 5113797 has a basic periodicity of 0.35 d with changing amplitude and shape of the light curve (Fig. 7). The high effective temperature (it is classified as A3) makes it unlikely to be a  $\gamma$  Dor variable. The star is 2XMMi J194212.3+401747 in the *XMM–Newton* Serendipitous Source Catalogue (Watson et al. 2009). The SC data show a very strong flare with height of 5 parts per thousand and complex decay (see Fig. 4).

There are a surprising number of other stars detected in the X-ray band. KIC 11189959 is the *ROSAT* source 1RXH J192628.4+485216 (ROSAT Scientific Team 2000). This star has the most peculiar light variation. There is a dominant 0.822-d period and its harmonic as well as a secondary 0.612-d period which has a low amplitude at first, but an increased amplitude at other times.

This is perhaps a binary system with the two periods being the rotational periods of the stars. There are a number of very strong flares in the SC data which are also clearly resolved in the LC data. Another *ROSAT* source, KIC 11137395 (1RXH J192709.8+484750), shows at least five strong flares in the SC data. The LC data show one strong resolved flare and several other weaker unresolved flares. The star has a period of 1.57 d with variable amplitude in the range 6–25 mmag.

Over 20 very strong flares are visible in the SC data of KIC 11551430, the *ROSAT* source 1RXS J190940.4+493004. The LC data show a large number of strong flares many of which are resolved or partially resolved. The star has a period of 4.19 d and variable amplitude in the range 9–65 mmag. In KIC 11560431 (*ROSAT* source 1RXS J193016.8+493156), at least 15 strong flares are seen in the SC data and a large number in the LC data, the strongest of which are resolved. The period is 3.14 d with variable amplitude in the range 9–40 mmag.

KIC 8703413, an Am star and *Chandra* X-ray source CXOX 194711.4+445054 (Flesch 2010), has a moderately strong and well-resolved flare in the SC data (Fig. 4) and hints of several other flares in the LC data. The period is 6.54 d with variable amplitude in the range 0.3–1.3 mmag. There is one other Am star which is an X-ray source: HR 8799 (Robrade & Schmitt 2010). We examined 10 other Am stars in the *Kepler* field, but could find no evidence of flares.

In KIC 9216367, an Ap star, the SC data show two moderate flares (Fig. 4) and indications of several unresolved weak flares in the LC data. The period is  $P = 3.250$  d with variable amplitude in the range 8–16 mmag. An Ap star normally shows a stable rotational light curve. The variable shape and amplitude suggests that it may not be an Ap star. Uytterhoeven et al. (2011) classify it as a  $\gamma$  Dor variable in an eclipsing binary, but the variable amplitude is not typical of an eclipsing binary. X-ray emission from Ap stars has recently been detected (Robrade & Schmitt 2011). We looked at six other known Ap stars in the *Kepler* field but could not detect any flares.

There are few eclipsing binaries in Tables 1–4. KIC 2557430 is a detached binary ( $P = 1.298$  d) with alternate depth of eclipses (43 and 33 mmag). In addition, there is an overall variability which may be due to starspots. There are a number of very large flares which are fully resolved in the SC data but only partially resolved in the LC data. In KIC 5263749, the double-wave nature of the light curve ( $P = 3.729$  d) could be interpreted as an interacting binary observed at a low inclination, but may equally well be explained by starspots. The peak-to-peak amplitude is only 2.5 mmag. The amplitude and shape are constant, which is unusual. Two clear flares can be seen in the SC data and a few additional flares in the LC data. KIC 4472809 appears to be an interacting binary with  $P = 2.361$  d, though it could also be interpreted as a spotted star. Three very large flares are resolved in the LC data. In KIC 5213466, an eclipsing binary with  $P = 2.82$  d, a few flares can be detected in the LC data.

In KIC 5733906 two flares are seen in the SC data. The LC data show some particularly large flares, one of them with relative intensity of 0.127. The star has been classified as an unknown type of pulsating variable: ASAS J195503+4055.3 (Pigulski et al. 2009) and HAT 199–13383 (Hartman et al. 2004). The light curve ( $P = 0.719$  d) shows large amplitude variations (54–110 mmag peak-to-peak) and migrating features more typical of a spotted star.

At least five strong flares are seen in the SC data of KIC 10459987 and a very large number in the LC data. The light curve is typical of migrating spots with variable amplitude in the range 12–35 mmag and a period of 6.02 d. This star, ASAS J190858+4741.1, is classified either as an unknown type of pulsating variable or as an

interacting binary (Pigulski et al. 2009). KIC 8351193 is a B9V star in which a moderate well-resolved flare can be seen (Fig. 4). The LC data indicate the presence of several other flares. The period is 0.57 d, but with extremely low amplitude ( $A = 2 \mu\text{mag}$ ).

KIC 7093428 shows at least a dozen very strong flares in the SC data and a great number of well-resolved flares in the LC data. KIC 9778156 has many strong flares. Several moderate flares can be seen in the LC data of the A-type stars KIC 3974751 and KIC 10489286. These four stars with frequent flares certainly deserve closer study.

We noted flares on three subdwarf B stars. In KIC 8142623 the SC data show one very strong flare, with a few poorly resolved strong flares in the LC data with indications of many smaller, unresolved flares. The amplitude is 15 mmag and the period, 1.118 d, may be the orbital period of a late-type companion. In KIC 10593239, two moderate flares are visible in the SC data and dozens more in the LC data. The period is 1.887 d with variable amplitude in the range 12–35 mmag. KIC 11350152 has a light curve which could be interpreted in terms of migrating starspots in a cool companion (Østensen et al. 2011) with a period of 3.159 d. Two weak flares are visible in the SC data and several others in the LC data.

#### 4 THE ORIGIN OF FLARES IN HOT STARS

Fig. 8 shows the location of the hot flare stars and the cool flare stars analysed by Walkowicz et al. (2011). They are scattered uniformly in luminosity and temperature. Many of the stars fall within the  $\delta$  Sct instability region, though Tables 1–4 contain only one  $\delta$  Sct variable. We do not understand why not more than half of the stars in the instability strip actually pulsate (Balona & Dziembowski 2011). The difficulty of detecting a flare in such variables has already been mentioned.

The first consideration that comes to mind is that flaring in a hot star may not be intrinsic to the star itself but may occur in a cool companion. This offers a simple explanation involving a known mechanism. Indeed, it is generally assumed that X-ray flares in A–F stars originate in a cool companion unless there is evidence to the contrary. One can reasonably assume that flare intensities on the cool companion are the same as in field stars of the same spectral type. Therefore, the relative flare intensities in the combined light of the two stars should be smaller than in isolated field stars.

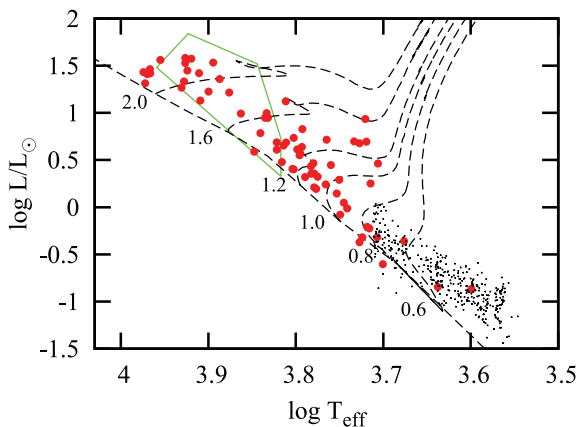


**Figure 8.** Location of hot flare stars (filled circles) in the theoretical Hertzsprung–Russell (HR) diagram. The cool flare stars in Walkowicz et al. (2011) are shown by small filled circles. The trapezoidal region is the general location of *Kepler*  $\delta$  Scuti stars (from Balona & Dziembowski 2011). Evolutionary tracks with indicated solar masses and of solar composition are from Bertelli et al. (2008).

The work of Walkowicz et al. (2011) on flares in *Kepler* cool dwarfs is particularly important in testing this hypothesis because it offers a benchmark on the relative peak flare intensities of K–M dwarfs using the same instrument and filter as used for the *Kepler* A–F stars discussed in this paper. Using the effective temperatures and radii listed in the KIC, we may derive the stellar luminosities for these stars. In Table 6, we show the mean stellar luminosities, flare EWs and relative flare intensities for K–M stars derived from table 2 of Walkowicz et al. (2011). We also show the same mean quantities for the stars of Tables 1–4. We have, however, omitted the three sdB stars as these are in a different state of evolution.

We note, in fact, that the relative flare intensities for single K–M stars is much the same as for the A–F stars. There is no decrease of flare intensities as might be expected if the flares originate in cool companions. There is, of course, a selection bias, since we can only observe flares with relative intensities exceeding some threshold (about  $10^{-4}$  for the *Kepler* stars). However, if anything, flares from field K–M stars should be biased towards higher intensities because these are considerably fainter than the A–F stars. Also many more K–M field flare stars were detected than A–F flare stars. We can therefore be sure that the mean peak flare intensity for these cool dwarfs is not an underestimate.

In Table 6 we show the mean EW,  $\log EW_c$ , and mean peak flare intensity,  $\log \Delta F/F_c$ , that might be expected in the combined light, using the mean peak values for the isolated cool flare stars shown in the first line of this table. The expected EW and relative intensities in combined light are about 30 times smaller than observed for F-type stars and about 100 times smaller than observed in A8–A0 stars. If flares originate in cool companions, then these flares must be about 30–100 times more intense than in cool flare stars in the general field. We do not know of any physical reason why this should be the case and we conclude that flares in F-type, and certainly in A-type stars cannot originate on cool companions.

The mean EW of flares in these stars is about  $3 \times 10^{-3}$  h. Since the luminosity of a typical A star is  $30 L_\odot$  or  $4 \times 10^{38}$  erg  $\text{h}^{-1}$ , the energy released in a typical flare is about  $10^{36}$  erg, or  $10^6$  times the energy of a large solar flare. Such a huge factor seems difficult to reconcile with the flare mechanism operating in the Sun and in cool flare stars. For the less luminous F stars, the flare energy would be about  $10^{35}$  erg.

We can estimate very crudely the magnetic field strength required to store the energy released in these intense flares. The energy stored in a magnetic field is proportional to the square of the field intensity. Since the flares on A-type stars are about  $10^6$  times more energetic than solar flares, the magnetic field intensity required to store this energy is about  $10^3$  times larger than in the Sun. Since the global solar magnetic field strength is about 1 G, a magnetic field of around 1000 G is required. Magnetic fields of this strength are known in Ap stars, but not in normal A-type stars. For example, the magnetic field in the A0 star Vega has a global intensity smaller than 1 G (Lignières et al. 2009).

It is possible that enough energy may be stored in a large number of magnetic ropes with high field strength, as in the Sun, but in this case one would still expect the resulting global field strength to be considerably higher than in the Sun. Furthermore, the low X-ray activity of A-type stars strongly suggests weak fields in these stars. Although strong magnetic fields can be generated through dynamo action in the convective core, the radiative envelope in A-type stars screens this strong field from the surface (Brun, Browning & Toomre 2005). The dynamo mechanism is not expected to be effective in the thin convection layer just below the photosphere of an A-type star.



**Table 6.** Mean luminosities, flare EWs and peak flare intensities ( $\Delta F/F$ ) for the cool M–K stars measured by Walkowicz et al. (2011) and for stars in Tables 1–4. The columns  $\log EW_c$  and  $\log \Delta F/F_c$  are the expected EWs and relative flare intensities assuming that the flare occurs on a M–K companion and is not intrinsic to the star.  $v_e$  is the mean equatorial rotational velocity ( $\text{km s}^{-1}$ ) derived from the stellar radii and photometric periods. The last column gives the mean equatorial rotational velocity for field giants and dwarfs in the given spectral type range.

Sp. type	$\log L/L_\odot$	$\log EW$	$\log \Delta F/F$	$\log EW_c$	$\log \Delta F/F_c$	$v_e$	$v_e$ field
M–K	$-0.74 \pm 0.02$	$-2.88 \pm 0.02$	$-2.48 \pm 0.02$				
G9–F9	$0.08 \pm 0.10$	$-1.96 \pm 0.17$	$-1.94 \pm 0.15$	–3.76	–3.36	$32 \pm 9$	$15 \pm 1$
F9–F5	$0.54 \pm 0.06$	$-2.89 \pm 0.13$	$-2.30 \pm 0.09$	–4.18	–3.78	$97 \pm 19$	$37 \pm 1$
F5–A8	$0.81 \pm 0.07$	$-2.61 \pm 0.30$	$-2.23 \pm 0.15$	–4.44	–4.04	$96 \pm 24$	$85 \pm 2$
A8–A0	$1.45 \pm 0.04$	$-2.56 \pm 0.19$	$-2.70 \pm 0.12$	–5.07	–4.67	$101 \pm 20$	$140 \pm 3$

The required magnetic field intensity can be reduced by increasing the volume in which it is contained. For example, magnetic field lines connecting an A-type star with a companion can be proposed as a possible solution to this problem. This mechanism has been suggested to explain intense flares in RS CVn stars (Simon et al. 1980; van den Oord 1988; Gunn et al. 1997). Magnetic fields linking two stars may be possible in the flaring A–F stars, though we have no direct evidence for companion stars except for the few eclipsing binaries. Measurements of magnetic field strengths in these stars should show higher fields than in other stars.

The idea that flares are caused by magnetic reconnection is reasonable because this is the mechanism thought responsible for solar flares. However, other mechanisms are possible, such as the release of kinetic energy by infalling bodies. If we assume a typical infall speed of  $100 \text{ km s}^{-1}$ , an energy release of  $10^{36} \text{ erg}$  requires a mass of about  $10^{22} \text{ g}$ . This roughly corresponds to bodies with typical sizes of 100–1000 km which may be plentiful around these relatively young stars. As an example of infalling bodies, we have  $\beta$  Pictoris, the prototype of an A-type star with a debris disc. High-resolution spectroscopic observations of the Ca II lines reveal variable absorption features which are always redshifted. These sporadic events have been interpreted as infalling comet-like bodies which evaporate when approaching the star (Lagrange, Ferlet & Vidal-Madjar 1987).

The typical interval between flares is a few tens of days. For an infalling body with mass  $10^{22} \text{ g}$ , one impact every 20 days for a million years translates into 100 000 times the mass of our Solar system’s asteroid belt. This mass is far too large to be acceptable. Although the idea that the flares are caused by infalling bodies is attractive because it does not disturb the current understanding of magnetic fields in A–F stars, it has to be rejected due to this reason. One could argue that the infall occurs only over a very short time, but this is likely only in the star’s infancy and none of the stars listed are known pre-main-sequence objects.

The significance that practically all A–F flare stars have well-defined photometric periods (see Fig. 7) is not clear, but seems to suggest that flaring may be related to starspots. We know that the dominant low frequency in A–F stars is the rotational frequency (Balona 2011), and we presume that the periods seen in the flare stars are the rotational periods. From the KIC radii of these stars and their photometric periods, we obtain the mean equatorial rotational velocities shown in Table 6. Also shown in the table are the mean equatorial rotational velocities for field dwarfs and giants in the given spectral type range. These are derived from the catalogue of projected rotational velocities (Glebocki & Stawikowski 2000) using the factor  $4/\pi$  to convert to mean equatorial velocities (Chandrasekhar & Münch 1950). There is no indication that the

flare stars are rotating more rapidly than stars of similar spectral type in the general field population.

Our conclusion is that flares in A–F stars, and particularly in A-type stars, cannot be ascribed to flaring in a cool companion. The huge energy in these flares cannot be stored in the typical magnetic field strengths observed in normal A-type stars. One possibility is that flare energy originates in magnetic reconnection of field lines spanning the A star and a companion. It is not known if this could be reconciled with the weak magnetic fields in these stars. The possibility that flares are caused by infalling comet-sized bodies is not supported by the typical flare frequency. This requires a vastly greater number of planetesimals than can be reasonably accommodated around these stars.

## 5 CONCLUSION

Optical flaring in hot F-type stars and in A-type stars has never been seen from the ground except in very few unverifiable cases. A-type stars have low X-ray activity with only 10–15 per cent of these being X-ray sources (Schröder & Schmitt 2007). A-type stars are thought not to have significant subsurface convection and cannot generate a magnetic field via the dynamo effect. This, in turn, prevents the formation of a corona and the stars are not expected to flare. Therefore, the source of the X-rays is usually attributed to an unseen cool companion.

Visual inspection of the SC and LC light curves of nearly 10 000 stars observed by *Kepler* show that, contrary to expectations, some early F- and A-type stars do flare. Flares are distinctly visible in 19 A8–A0 stars out of a total of 1883 *Kepler* stars in this spectral type range. Although this constitutes only 1 per cent of the number of A-type stars in the *Kepler* field, it should be borne in mind that only those stars with the most intense and more frequent flares are likely to have been detected and that a considerably larger fraction of A-type stars may possibly flare.

We used the peak flare intensities and EWs of 373 *Kepler* K–M stars by Walkowicz et al. (2011) to establish the mean peak intensity and EW that one may expect on a cool companion to an A-type star. It turns out that the expected flare intensity and EW in the combined light of an A star and a cool companion is about 100 times smaller than observed. We therefore conclude that it is unlikely that flares in A-type stars can be attributed to cool companions.

We estimate that the energy released in flares on A-type stars is about  $10^{36} \text{ erg}$ . The weak magnetic fields that have been observed in normal A-type stars are incapable of storing this energy. It may be possible to release this energy in a magnetic field connecting the A star with a companion, but this idea requires further study. It would be important to determine if any of the A-type flare stars have measurable magnetic fields. The kinetic energy released by

infalling planetesimals with typical sizes in the range 100–1000 km was considered as a possible explanation for the flares, but the typical flaring rate implies a reservoir of planetesimals far too large to be acceptable.

It is tempting to consider the A–F flare stars to be the low-energy end of the ‘superflare’ stars (Schaefer 1989; Schaefer et al. 2000). This may be the case, but one needs to bear in mind that some of the superflares have amplitudes measured in magnitudes, whereas the flares discussed here are measured in millimagnitudes. To some extent this may be a consequence of the different passbands, since the white-light passband in *Kepler* greatly suppresses the amplitude relative to blue-light observations.

Whatever the correct explanation may turn out to be, these stars certainly deserve further attention. Spectroscopic monitoring may be able to confirm the presence of infalling bodies. In some stars, the presumed rotational modulation due to starspots should lead to observable line profile variations. Stars with frequent flares deserve particular attention as these offer the possibility of a spectrum when a flare is present.

## ACKNOWLEDGMENTS

This paper includes data collected by the *Kepler* mission. Funding for the *Kepler* mission is provided by the NASA Science Mission directorate. The authors wish to thank the *Kepler* team for their generosity in allowing the data to be released and for their outstanding efforts which have made these results possible.

All of the data presented in this paper were obtained from the Multimission Archive at the Space Telescope Science Institute (MAST). STScI is operated by the Association of Universities for Research in Astronomy, Inc., under NASA contract NAS5-26555. Support for MAST for non-*HST* data is provided by the NASA Office of Space Science via grant NNX09AF08G and by other grants and contracts.

LAB wishes to thank the South African Astronomical Observatory and the National Research Foundation for financial support.

## REFERENCES

- Balona L. A., 2011, *MNRAS*, 415, 1691  
 Balona L. A., Dziembowski W. A., 2011, *MNRAS*, 417, 591  
 Balona L. A., Guzik J. A., Uytterhoeven K., Smith J. C., Tenenbaum P., Twicken J. D., 2011, *MNRAS*, 415, 3531  
 Bell B., Glazer H., 1959, *Smithsonian Contr. Astrophys.*, 3, 25  
 Benz A. O., Güdel M., 2010, *ARA&A*, 48, 241  
 Berghoefer T. W., Schmitt J. H. M. M., 1994, *Ap&SS*, 221, 309  
 Bertelli G., Girardi L., Marigo P., Nasi E., 2008, *A&A*, 484, 815  
 Biermann L., 1948, *Z. Astrophys.*, 25, 135  
 Brown T. M., Latham D. W., Everett M. E., Esquerdo G. A., 2011, *AJ*, 142, 112  
 Brun A. S., Browning M. K., Toomre J., 2005, *ApJ*, 629, 461  
 Chandrasekhar S., Münch G., 1950, *ApJ*, 111, 142  
 Cuntz M., Saar S. H., Musielak Z. E., 2000, *ApJ*, 533, L151  
 Degroote P. et al., 2009, *A&A*, 506, 471  
 Flesch E., 2010, *Publ. Astron. Soc. Australia*, 27, 283  
 Gilliland R. L. et al., 2010, *ApJ*, 713, L160  
 Glebocki R., Stawikowski A., 2000, *Acta Astron.*, 50, 509  
 Güdel M., Nazé Y., 2009, *A&AR*, 17, 309  
 Gunn A. G., Migenes V., Doyle J. G., Spencer R. E., Mathioudakis M., 1997, *MNRAS*, 287, 199  
 Hartman J. D., Bakos G., Stanek K. Z., Noyes R. W., 2004, *AJ*, 128, 1761  
 Hubrig S., Marco O., Stelzer B., Schöller M., Huéramo N., 2007, *MNRAS*, 381, 1569  
 Ip W.-H., Kopp A., Hu J.-H., 2004, *ApJ*, 602, L53  
 Jenkins J. M. et al., 2010, *ApJ*, 713, L120  
 Kretzschmar M., 2011, *A&A*, 530, A84  
 Lagrange A. M., Ferlet R., Vidal-Madjar A., 1987, *A&A*, 173, 289  
 Lanza A. F., 2008, *A&A*, 487, 1163  
 Lanza A. F., Rodono M., Zappala R. A., 1993, *A&A*, 269, 351  
 Lignières F., Petit P., Böhm T., Aurière M., 2009, *A&A*, 500, L41  
 Mathioudakis M., Doyle J. G., Avgoloupis V., Mavridis L. N., Seiradakis J. H., 1992, *MNRAS*, 255, 48  
 Miura J., Tsujimoto M., Tsuboi Y., Maeda Y., Sugawara Y., Koyama K., Yamauchi S., 2008, *PASJ*, 60, 49  
 Mullan D. J., Mathioudakis M., 2000, *ApJ*, 544, 475  
 Østensen R. H. et al., 2011, *MNRAS*, 414, 2860  
 Pigulski A., Pojmański G., Pilecki B., Szczygieł D. M., 2009, *Acta Astron.*, 59, 33  
 Pinsonneault M. H., An D., Molenda-Żakowicz J., Chaplin W. J., Metcalfe T. S., Bruntt H., 2012, *ApJS*, 199, 30  
 Robrade J., Schmitt J. H. M. M., 2009, *A&A*, 497, 511  
 Robrade J., Schmitt J. H. M. M., 2010, *A&A*, 516, A38  
 Robrade J., Schmitt J. H. M. M., 2011, *A&A*, 531, A58  
 ROSAT Scientific Team, 2000, *VizieR Online Data Catalog*, 9028, 0  
 Rubenstein E. P., Schaefer B. E., 2000, *ApJ*, 529, 1031  
 Schaefer B. E., 1989, *ApJ*, 337, 927  
 Schaefer B. E., 1991, *ApJ*, 366, L39  
 Schaefer B. E., King J. R., Deliyannis C. P., 2000, *ApJ*, 529, 1026  
 Schmitt J. H. M. M., Guedel M., Predehl P., 1994, *A&A*, 287, 843  
 Schröder C., Schmitt J. H. M. M., 2007, *A&A*, 475, 677  
 Simon T., Linsky J. L., Schiffer F. H., III, 1980, *ApJ*, 239, 911  
 Strassmeier K. G., 2009, *A&AR*, 17, 251  
 Strassmeier K. G., Bopp B. W., 1992, *A&A*, 259, 183  
 Uytterhoeven K. et al., 2011, *A&A*, 534, A125  
 van den Oord G. H. J., 1988, *A&A*, 205, 167  
 Walkowicz L. M. et al., 2011, *AJ*, 141, 50  
 Wang J., 1993, *Inf. Bull. Var. Stars*, 3836, 1  
 Watson M. G. et al., 2009, *A&A*, 493, 339  
 Yanagida T., Ezoe Y. I., Makishima K., 2004, *PASJ*, 56, 813  
 Yanagida T., Ezoe Y., Kawaharada M., Kokubun M., Makishima K., 2007, in Okazaki A. T., Owocki S. P., Stefl S., eds, *ASP Conf. Ser. Vol. 361, Active OB-Stars: Laboratories for Stellar and Circumstellar Physics*. Astron. Soc. Pac., San Francisco, p. 533

This paper has been typeset from a  $\text{\TeX}/\text{\LaTeX}$  file prepared by the author.